

# Multijet and multi-differential dijet measurements with ATLAS and CMS

Argyro Ziaka

On behalf of ATLAS and CMS collaborations

University of Ioannina

QCD@LHC 2024

Monday 7<sup>th</sup> October 2024



## 1 Motivation

## 2 ATLAS measurements

- (Azimuthal Asymmetry) Transverse Energy-Energy Correlations<sup>1</sup>
- Jet cross section ratios<sup>2</sup>

## 3 CMS measurements

- Azimuthal correlations ( $R_{\Delta\phi}$ )<sup>3</sup>
- Multi-differential dijet cross sections<sup>4</sup>

## 4 Summary & Conclusions

---

<sup>1</sup> JHEP 07 (2023) 85

<sup>2</sup> arXiv:2405.20206, submitted to PRD

<sup>3</sup> EPJC 84, 842 (2024)

<sup>4</sup> arXiv:2312.16669, submitted to EPJC

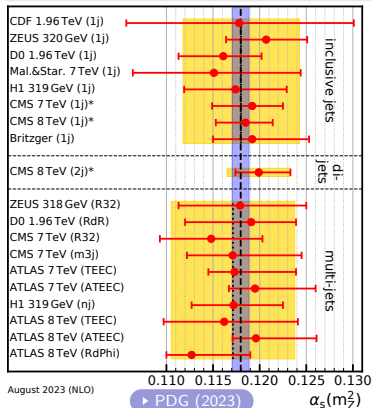
# Motivation

## Jet measurements

- Study of QCD (precision measurements)
- Extraction of  $\alpha_S(m_Z)$ , running of  $\alpha_S(Q)$
- Tune Monte Carlo event generators
- Constrain Parton Distribution Functions

## In this presentation

Run 2 analyses are discussed



# Motivation

## Jet measurements

- Study of QCD (precision measurements)
- Extraction of  $\alpha_S(m_Z)$ , running of  $\alpha_S(Q)$
- Tune Monte Carlo event generators
- Constrain Parton Distribution Functions

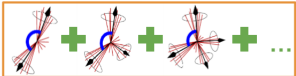
## Multijet cross section ratios

- Determination of the strong coupling constant  $\alpha_S(m_Z)$
- Investigation of  $\alpha_S$  running in TeV scale

# Motivation

## Jet measurements

- Study of QCD (precision measurements)
- Extraction of  $\alpha_S(m_Z)$ , running of  $\alpha_S(Q)$
- Tune Monte Carlo event generators
- Constrain Parton Distribution Functions

$$\mathbf{R} = \frac{\text{[Diagram of jet topologies]}}{\text{[Diagram of jet topologies]}}$$


## Multijet cross section ratios

- Determination of the strong coupling constant  $\alpha_S(m_Z)$
- Investigation of  $\alpha_S$  running in TeV scale

In ratios ( $\mathbf{R}$ ) with

- **Denominator: topologies with at least 2-jets ( $\sim \alpha_S^2$  @LO)**

# Motivation

## Jet measurements

- Study of QCD (precision measurements)
- Extraction of  $\alpha_S(m_Z)$ , running of  $\alpha_S(Q)$
- Tune Monte Carlo event generators
- Constrain Parton Distribution Functions

$$\mathbf{R} = \frac{\boxed{\text{diagram 1}} + \boxed{\text{diagram 2}} + \dots}{\boxed{\text{diagram 3}} + \boxed{\text{diagram 4}} + \boxed{\text{diagram 5}} + \dots}$$

The diagram shows the ratio  $\mathbf{R}$  as a fraction. The numerator is enclosed in a blue box and contains two diagrams of a quark-gluon jet with a blue circle around the quark line, followed by a plus sign and another similar diagram, and an ellipsis. The denominator is enclosed in an orange box and contains three such diagrams, followed by a plus sign and another, and an ellipsis.

## Multijet cross section ratios

- Determination of the strong coupling constant  $\alpha_S(m_Z)$
- Investigation of  $\alpha_S$  running in TeV scale

In ratios ( $\mathbf{R}$ ) with

- **Denominator:** topologies with at least 2-jets ( $\sim \alpha_s^2$  @LO)
- **Numerator:** topologies with at least 3-jets ( $\sim \alpha_s^3$  @LO)

# Motivation

## Jet measurements

- Study of QCD (precision measurements)
- Extraction of  $\alpha_S(m_Z)$ , running of  $\alpha_S(Q)$
- Tune Monte Carlo event generators
- Constrain Parton Distribution Functions

$$\mathbf{R} = \frac{\boxed{\text{diagram 1}} + \boxed{\text{diagram 2}} + \dots}{\boxed{\text{diagram 3}} + \boxed{\text{diagram 4}} + \boxed{\text{diagram 5}} + \dots}$$

The diagram shows a ratio  $\mathbf{R}$  of two sums of jet topologies. The numerator (top row, blue border) contains two diagrams of a quark-gluon jet with a blue circle around the quark line, followed by a plus sign, another similar diagram, another plus sign, and an ellipsis. The denominator (bottom row, orange border) contains three similar diagrams, followed by plus signs and an ellipsis.

## Multijet cross section ratios

- Determination of the strong coupling constant  $\alpha_S(m_Z)$
- Investigation of  $\alpha_S$  running in TeV scale

In ratios ( $\mathbf{R}$ ) with

- **Denominator:** topologies with at least 2-jets ( $\sim \alpha_s^2$  @LO)
- **Numerator:** topologies with at least 3-jets ( $\sim \alpha_s^3$  @LO)

**Benefits**

- ✓ Cancellation of systematic effects e.g. luminosity
- ✓ Reduction of theoretical uncertainties e.g. non-perturbative

- Transverse Energy-Energy Correlations (TEEC)

$$\frac{1}{\sigma} \frac{d\Sigma}{d \cos \phi} = \frac{1}{N} \sum_{A=1}^N \sum_{ij} \frac{E_{T_i}^A E_{T_j}^A}{(\sum_k E_{T_k}^A)^2} \delta(\cos \phi - \cos \phi_{ij})$$

- Normalised to  $\sigma$
- Weighted by  $E_T = \frac{E}{\cosh y}$
- $i, j, k$ : indices over all jets
- $\phi_{ij}$ : angle in transverse plane
- $N$  multijet events
- $\delta(x)$ : Dirac function  $\rightarrow \phi = \phi_{ij}$



# ATLAS - TEEC: Samples and event selection

- Associated azimuthal (A)symmetries of (A)TEEC
- Cancel uncertainties symmetric in  $\cos \phi$
- Difference between  $\cos \phi > 0$  and  $\cos \phi < 0$  of TEEC:

$$\frac{1}{\sigma} \frac{d\Sigma^{asym}}{d \cos \phi} = \frac{1}{\sigma} \left. \frac{d\Sigma}{d \cos \phi} \right|_{\phi} - \frac{1}{\sigma} \left. \frac{d\Sigma}{d \cos \phi} \right|_{\pi-\phi}$$

- TEEC and ATEEC sensitive to gluon radiation and  $\alpha_S$
-

# ATLAS - TEEC: Samples and event selection

- Associated azimuthal (A)symmetries of (A)TEEC
- Cancel uncertainties symmetric in  $\cos\phi$
- Difference between  $\cos\phi > 0$  and  $\cos\phi < 0$  of TEEC:

$$\frac{1}{\sigma} \frac{d\Sigma^{asym}}{d\cos\phi} = \frac{1}{\sigma} \left. \frac{d\Sigma}{d\cos\phi} \right|_{\phi} - \frac{1}{\sigma} \left. \frac{d\Sigma}{d\cos\phi} \right|_{\pi-\phi}$$

- TEEC and ATEEC sensitive to gluon radiation and  $\alpha_S$

## Data

Full Run 2 (2015-2018)

→  $\sqrt{s} = 13$  TeV,  $\mathcal{L}_{int} = 139$  fb $^{-1}$

## Jet reconstruction (FASTJET)

- **Jet algorithm:** anti- $k_T$
- **Jet size:** R=0.4

## Event selection

- Select high- $p_T$  jets:
  - Single-jet trigger minimum threshold:  $p_T = 460$  GeV
- Phase-space selection:
  - $p_T > 60$  GeV
  - $|y| < 2.4$
  - $H_{T2} = p_{T1} + p_{T2} > 1$  TeV for 2 leading jets, in bins of  $H_{T2}$

# ATLAS - TEEC: Unfolding and Systematic uncertainties

- Unfolding using iterative algorithm based on Bayesian theorem
- Parametrise probability of gen jet in bin  $i \rightarrow$  rec in bin  $j$  :  $M_{ij}$  transfer matrix (from MC)
- Inverse problem:  $\mathcal{R}_i = \sum_{j=1}^N \frac{\mathcal{E}_j}{\mathcal{P}_i} M_{ij} T_j$ ,  $\mathcal{E}_j(\mathcal{P}_i)$ : efficiency(purity) corrections
- $\mathcal{R}_i(T_j)$ : content of detector(particle) level distribution in bin  $i(j)$

# ATLAS - TEEC: Unfolding and Systematic uncertainties

- Unfolding using iterative algorithm based on Bayesian theorem
- Parametrise probability of gen jet in bin  $i \rightarrow$  rec in bin  $j$ :  $M_{ij}$  transfer matrix (from MC)
- Inverse problem:  $\mathcal{R}_i = \sum_{j=1}^N \frac{\mathcal{E}_j}{\mathcal{P}_i} M_{ij} T_j$ ,  $\mathcal{E}_j(\mathcal{P}_i)$ : efficiency(purity) corrections
- $\mathcal{R}_i(T_j)$ : content of detector(particle) level distribution in bin  $i(j)$

**Total: 0.5-3.2%**

**Modelling: 1.5-2%**

**Unfolding:  $\approx 0\%$**

**JES: 0.5-2.5%**

**JER:  $\approx 0.25\%$**

**JAR  $< 0.5\%$**

**Total: 0.5-1.3%**

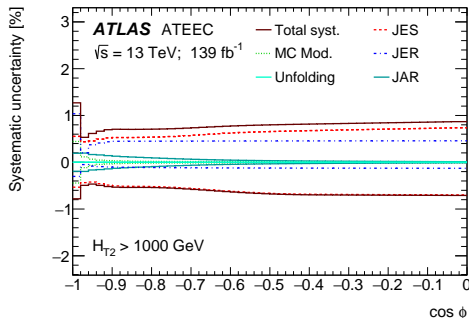
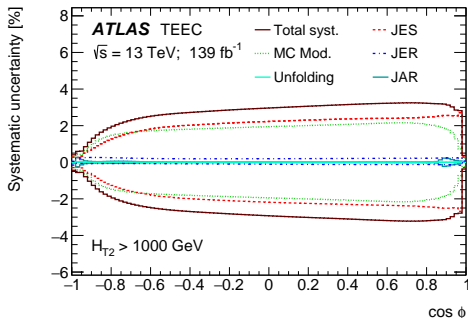
**Modelling:  $< 0.5\%$**

**Unfolding:  $\approx 0\%$**

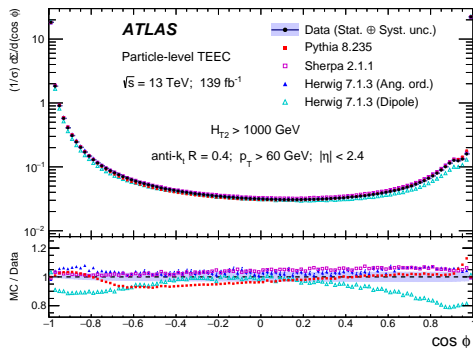
**JES: 0.4-0.7%**

**JER:  $< 1\%$**

**JAR  $< 0.5\%$**

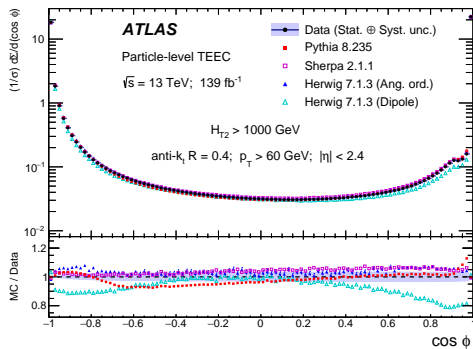


# ATLAS - (A)TEEC: Experimental results



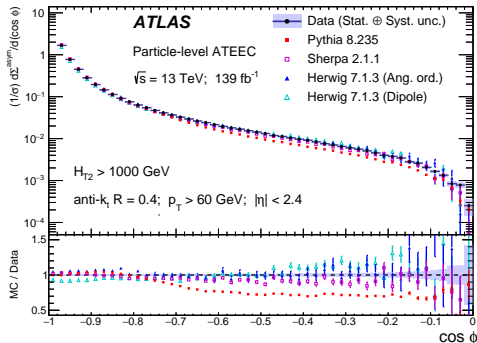
- Two peaks:  $\cos \phi = -1, 1$
- Central plateau: wide-angle radiation
- Kink: dependence on  $R$
- Best description:  
SHERPA and HERWIG7

# ATLAS - (A)TEEC: Experimental results

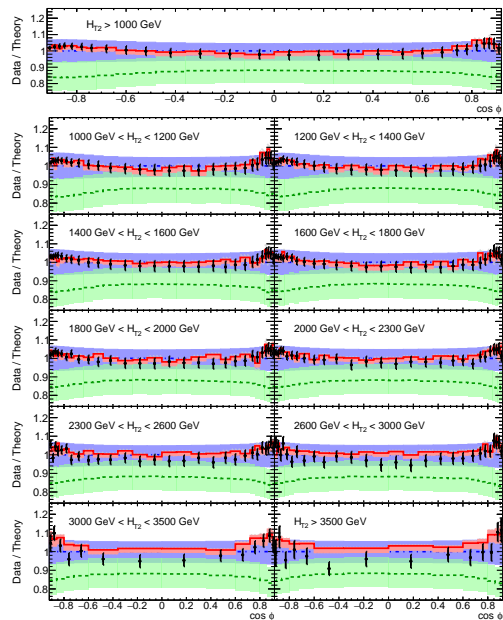


- Steeply falling distributions by several orders of magnitude
- Best description by **SHERPA** and **HERWIG7**

- Two peaks:  $\cos \phi = -1, 1$
- Central plateau: wide-angle radiation
- Kink: dependence on  $R$
- Best description:  
**SHERPA** and **HERWIG7**



# ATLAS - TEEC: Fixed-order pQCD



**ATLAS**

Particle-level TEEC

$\sqrt{s} = 13 \text{ TeV}; 139 \text{ fb}^{-1}$

anti- $k_T$   $R = 0.4$

$p_{T,1} > 60 \text{ GeV}$

$|\eta| < 2.4$

$\mu_{R,F} = \hat{p}_T$

$\alpha_s(m_Z) = 0.1180$

MMHT 2014 (NNLO)

— Data  
- - - LO  
- · - NLO  
- - - NNLO

► PRL 127(2021) 152001

Predictions up to **NNLO**

# ATLAS - TEEC: Fixed-order pQCD

► PRL 127(2021) 152001

Predictions up to **NNLO**

**ATLAS**

Particle-level TEEC

$\sqrt{s} = 13 \text{ TeV}; 139 \text{ fb}^{-1}$

anti- $k_T$   $R = 0.4$

$p_{T,1} > 60 \text{ GeV}$

$|\eta| < 2.4$

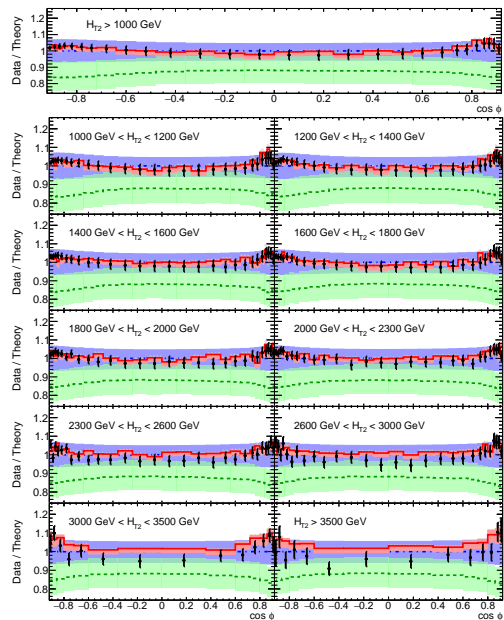
$\mu_{R,F} = \hat{p}_T$

$\alpha_s(m_Z) = 0.1180$

MMHT 2014 (NNLO)

— Data  
- - - LO  
- · - NLO  
- - - NNLO

← Improved scale uncertainties  
(dominant)





# ATLAS - TEEC: Fixed-order pQCD

► PRL 127(2021) 152001

Predictions up to **NNLO**

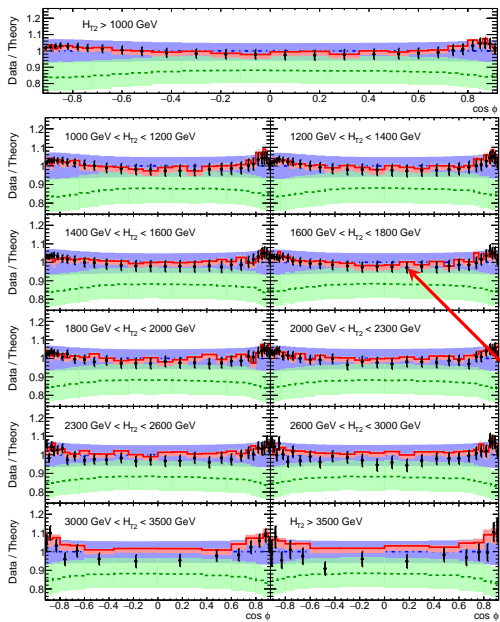
**ATLAS**  
Particle-level TEEC  
 $\sqrt{s} = 13 \text{ TeV}; 139 \text{ fb}^{-1}$

anti- $k_t$   $R = 0.4$   
 $p_T > 60 \text{ GeV}$   
 $|\eta| < 2.4$   
 $\mu_{R,F} = \hat{p}_T$   
 $\alpha_s(m_Z) = 0.1180$

MMHT 2014 (NNLO)  
— Data  
- - - LO  
- · - NLO  
- - - NNLO

Nice Data - **Theory** agreement

← Agreement within uncertainties



# ATLAS - TEEC: Fixed-order pQCD

► PRL 127(2021) 152001

Predictions up to **NNLO**

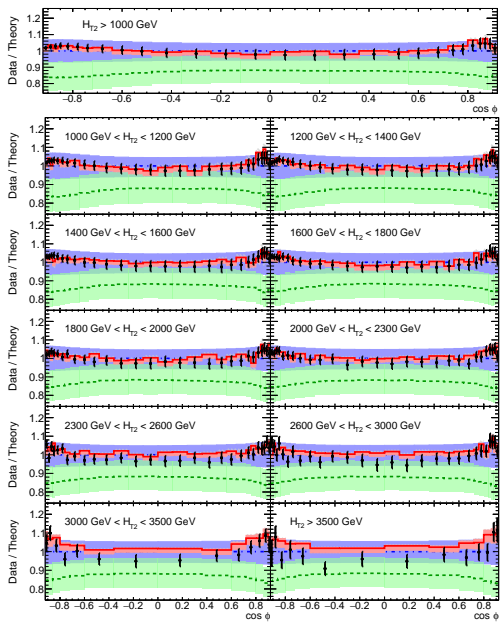
**ATLAS**  
 Particle-level TEEC  
 $\sqrt{s} = 13 \text{ TeV}; 139 \text{ fb}^{-1}$

anti- $k_T$   $R = 0.4$   
 $p_{T,1} > 60 \text{ GeV}$   
 $|\eta| < 2.4$   
 $\mu_{R,F} = \hat{p}_T$   
 $\alpha_s(m_Z) = 0.1180$

MMHT 2014 (NNLO)  
 — Data  
 - - - LO  
 - · - NLO  
 — NNLO

■ TEEC:  
 $\alpha_s(m_Z) = 0.1175 \pm 0.0006(\text{exp.})_{-0.0017}^{+0.0034}(\text{th.})$

■ ATEEC:  
 $\alpha_s(m_Z) = 0.1185 \pm 0.0009(\text{exp.})_{-0.0012}^{+0.0025}(\text{th.})$



## Measurement

- Differential cross sections of multijet events
- Ratios between different inclusive jet-multiplicity bins e.g.

$$(R_{32} = \frac{3\text{-jet}}{2\text{-jet}}, R_{42} = \frac{4\text{-jet}}{2\text{-jet}}, R_{43} = \frac{4\text{-jet}}{3\text{-jet}}, R_{54} = \frac{5\text{-jet}}{4\text{-jet}})$$

## Measurement

- Differential cross sections of multijet events
- Ratios between different inclusive jet-multiplicity bins e.g.

$$(R_{32} = \frac{3\text{-jet}}{2\text{-jet}}, R_{42} = \frac{4\text{-jet}}{2\text{-jet}}, R_{43} = \frac{4\text{-jet}}{3\text{-jet}}, R_{54} = \frac{5\text{-jet}}{4\text{-jet}})$$

## Variables sensitive to energy scale

- $H_{T2} = p_{T,1} + p_{T,2}$ , if 3<sup>rd</sup> jet exists: varying  $p_{T,3}$  thresholds to understand resummation effects
- $p_T^{N_{incl}}$ : inclusive jet  $p_T$  in bins of multiplicity

## Measurement

- Differential cross sections of multijet events
- Ratios between different inclusive jet-multiplicity bins e.g.

$$(R_{32} = \frac{3\text{-jet}}{2\text{-jet}}, R_{42} = \frac{4\text{-jet}}{2\text{-jet}}, R_{43} = \frac{4\text{-jet}}{3\text{-jet}}, R_{54} = \frac{5\text{-jet}}{4\text{-jet}})$$

## Variables sensitive to energy scale

- $H_{T2} = p_{T,1} + p_{T,2}$ , if 3<sup>rd</sup> jet exists: varying  $p_{T,3}$  thresholds to understand resummation effects
- $p_T^{N_{incl}}$ : inclusive jet  $p_T$  in bins of multiplicity

## Variables sensitive to topology:

- Leading jets in the event:
  - $\Delta y_{jj}$ : absolute value of rapidity difference
  - $m_{jj}$ : invariant mass
- All selected jets in the event:
  - $\Delta y_{jj,max}$ : absolute value of rapidity difference
  - $m_{jj,max}$ : maximum dijet invariant mass

# ATLAS - Cross section ratios: Samples and event selection

## Data

**Full Run 2 (2015-2018)**

→  $\sqrt{s} = 13 \text{ TeV}$ ,  $\mathcal{L}_{int} = 139 \text{ fb}^{-1}$

## Jet reconstruction (FASTJET)

- **Jet algorithm:** anti- $k_T$
- **Jet size:**  $R=0.4$

# ATLAS - Cross section ratios: Samples and event selection

## Data

Full Run 2 (2015-2018)

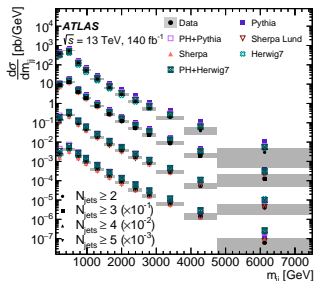
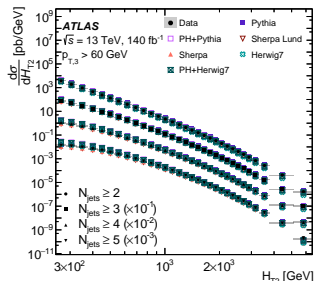
$\rightarrow \sqrt{s} = 13 \text{ TeV}, \mathcal{L}_{int} = 139 \text{ fb}^{-1}$

## Jet reconstruction (FASTJET)

- Jet algorithm: anti- $k_T$
- Jet size:  $R=0.4$

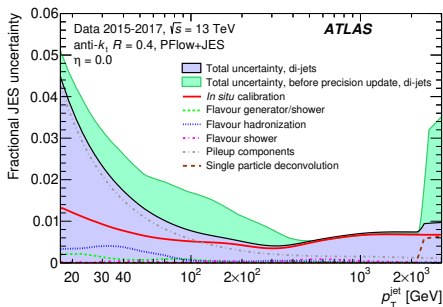
## Event selection

- Kinematic selection criteria to eliminate PU interactions:
  - $p_T > 60 \text{ GeV}$
  - $|y| < 4.5$
- Phase-space selection:
  - $N_{jets} \geq 2$
  - $H_{T2} = p_{T1} + p_{T2} \geq 250 \text{ GeV}$  for leading & sub-leading jets



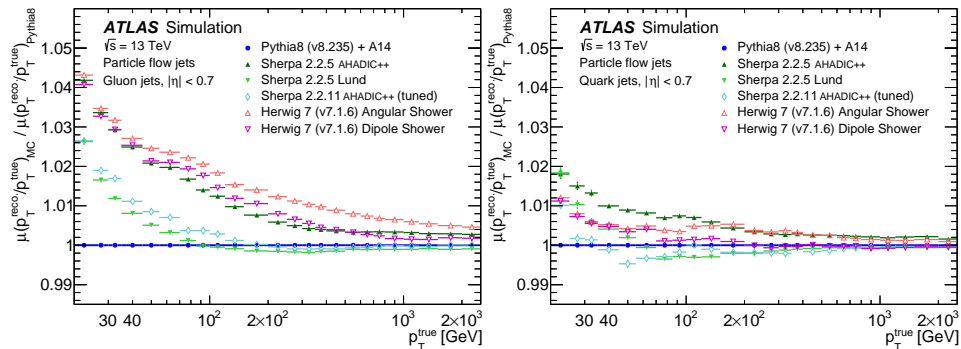
# ATLAS - Cross section ratios: Precision study

- Jet energy scale calibration:
  - ➔ Dominant systematic uncertainty source
- Precision improvements:
  - ➔ Jet flavor response dependence
  - ➔ Single hadron response extrapolation to jets
- Significant reduction of JES



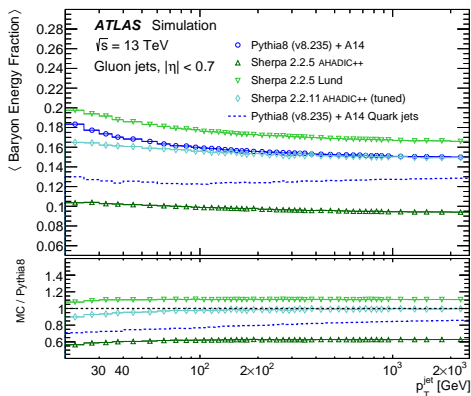


# ATLAS - Cross section ratios: Jet flavor response



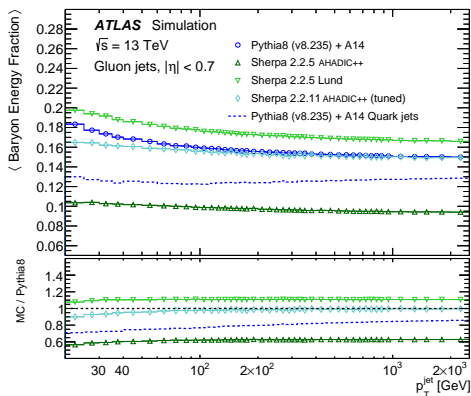
- Parton that initiated jet determines its internal dynamics
- Jet flavor response: uncertainty of actual spectra from data and relationship with JES
- Gluon-initiated jets (left): differences up to 4% with **PYTHIA**
- Quark-initiated jets (right): differences up to 1.8% with **PYTHIA**

# ATLAS - Cross section ratios: Jet flavor response

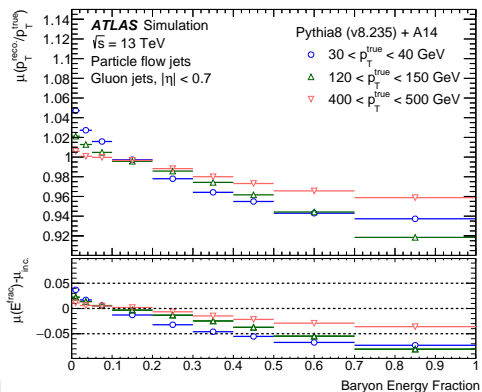


- Baryon energy fraction for **PYTHIA**: shown to illustrate the size of possible differences due to jet flavor
- For **SHERPA** with cluster hadronisation: lower energy fraction by baryons than **PYTHIA**

# ATLAS - Cross section ratios: Jet flavor response



- Baryon energy fraction for **PYTHIA**: shown to illustrate the size of possible differences due to jet flavor
- For **SHERPA** with cluster hadronisation: lower energy fraction by baryons than **PYTHIA**



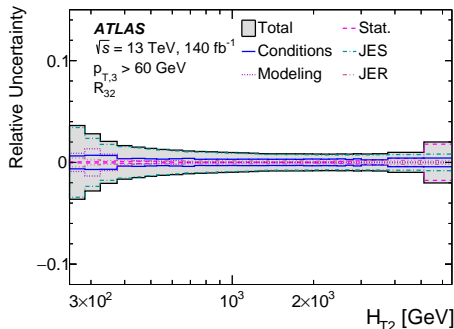
- Larger baryon energy fractions → lower response
- Most baryons: (anti-)protons and (anti-)neutrons

# ATLAS - Cross section ratios: Jet flavor response

- Jet flavor response previously taken by plain comparison between PYTHIA8 and HERWIG++
- Split into three separate uncertainty components by comparing different aspects of MC generator setups:
  - **Flavor generator/shower:** PYTHIA8 vs. SHERPA 2.2.5 w/ Lund string hadronisation
  - **Flavor hadronisation:** SHERPA 2.2.11 w/ AHADIC cluster-based hadronization vs. SHERPA 2.2.5 w/ Lund string hadronisation
  - **Flavor shower:** HERWIG 7.1 w/ angle-ordered PS vs. HERWIG 7.1 w/ dipole PS
- Uncertainties derived separately for five different jet flavors ( $u$  or  $d$ , and  $s$ ,  $c$ ,  $b$  and  $g$ ) and applied according to jet label in simulated event samples
- **Subdominant effect of final uncertainty compared to the initial leading contribution of jet flavor response**

# ATLAS - Cross section ratios: Unfolding and Exp. uncert.

- Statistical uncertainties arise from finite MC and Data sample size
- Treated during unfolding:
  - 1 Replicas of measured spectra are created containing Poisson-distributed fluctuations around nominal distributions
  - 2 Response Matrix is varied using these pseudo-experiments
  - 3 Replicas unfolded with varied RM  $\rightarrow$  replicas of unfolded spectra
  - 4 Statistical uncertainty: standard deviation of replicas



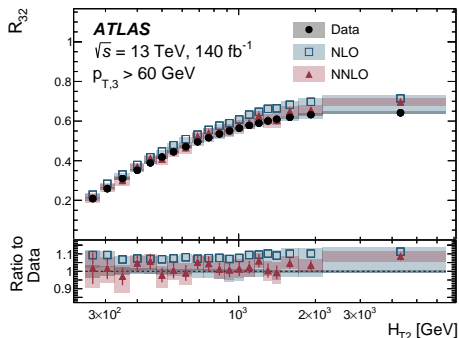
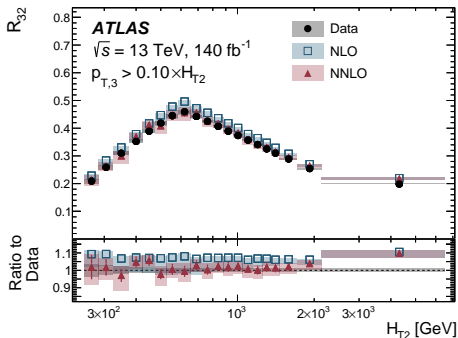
- 2D Unfolding (ROOUNFOLD):  
observable bins and exclusive  $N_{jets}$
- 3D for varied  $p_{T,3}$  :  $H_{T2}, N_{jets}, p_{T,3}$
- Recombination of exclusive  
 $\rightarrow$  inclusive  $N_{jets}$  distributions

**Tot:** 1-4.5%    **Stat:** < 1%  
**Cond:** < 2%    **JES:** 1-3.5%  
**Model:** < 1%    **JER:** < 1%

# ATLAS - Cross section ratios: Fixed-order pQCD

## Theoretical predictions

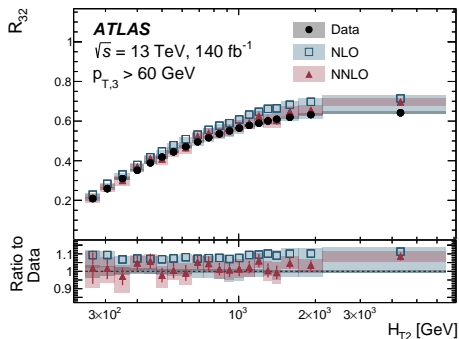
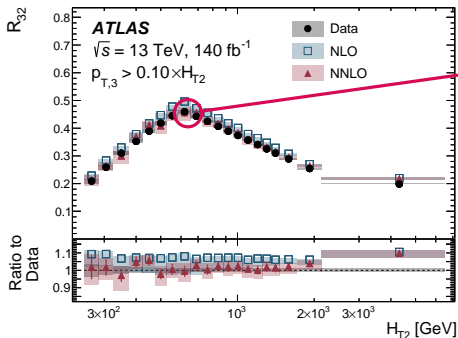
- 2- and 3-jet cross sections (NLO and NNLO)
- **PDF set:** MSHT20
- $\mu_r = \mu_f = \hat{H}_T = \sum_{i \in \text{partons}} p_{T,i}$
- $R_{32}(\text{NNLO}) = \frac{3\text{-jet (NNLO)}}{2\text{-jet (NNLO)}}$



# ATLAS - Cross section ratios: Fixed-order pQCD

## Theoretical predictions

- 2- and 3-jet cross sections (NLO and NNLO)
- **PDF set:** MSHT20
- $\mu_r = \mu_f = \hat{H}_T = \sum_{i \in \text{partons}} p_{T,i}$
- $R_{32}(\text{NNLO}) = \frac{3\text{-jet (NNLO)}}{2\text{-jet (NNLO)}}$

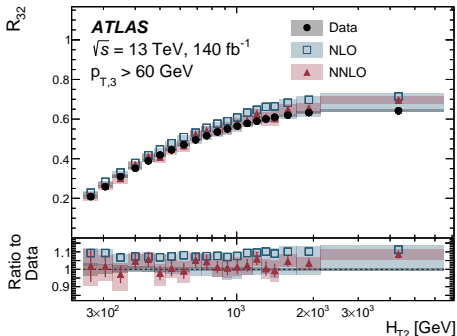
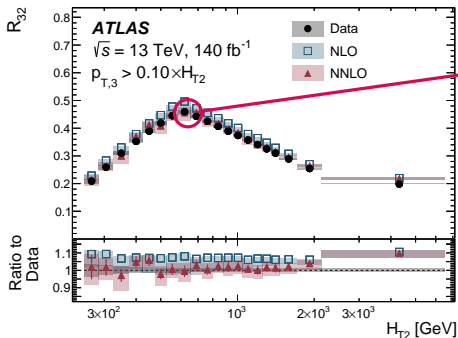


Peak dependent on  $p_{T,3}$  cut

# ATLAS - Cross section ratios: Fixed-order pQCD

## Theoretical predictions

- 2- and 3-jet cross sections (NLO and NNLO)
- **PDF set:** MSHT20
- $\mu_r = \mu_f = \hat{H}_T = \sum_{i \in \text{partons}} p_{T,i}$
- $R_{32}(\text{NNLO}) = \frac{3\text{-jet (NNLO)}}{2\text{-jet (NNLO)}}$



Peak dependent on  $p_{T,3}$  cut

**NLO prediction:** overestimates  $R_{32}$

► PRL 127(2021) 152001

**NNLO prediction:**

- ➔ Reduced scale uncertainty
- ➔ Nice agreement between Data and Theory

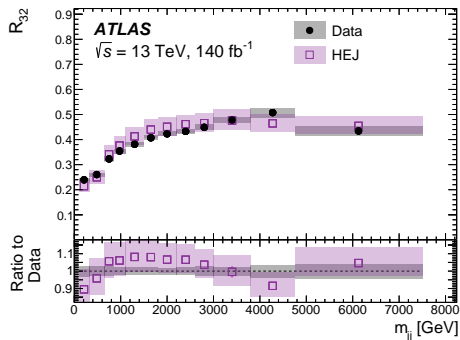
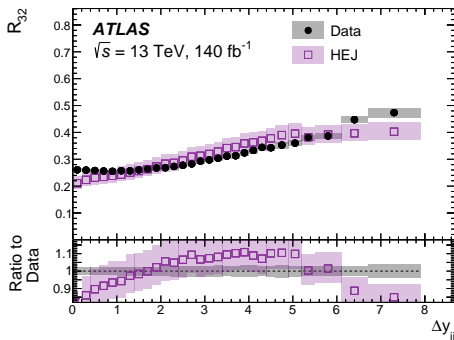


# ATLAS - Cross section ratios: Fixed-order pQCD

► JHEP 01(2010) 039

## ■ High Energy Jets (HEJ) framework


- Leading logarithmic QCD corrections in  $\hat{s}/p_T^2$ , all orders of  $\alpha_S$  and SM processes
- Resummation of logarithmic correction and matching to fixed-order accuracy:  $pp \rightarrow 2j, 3j, 4j, 5j, 6j$  at tree-level
- $\mu_r = \mu_f = \hat{H}_T/2$
- **PDF set:** NNPDF3.1NLO,  $\alpha_S(m_Z) = 0.118$



# CMS - $R_{\Delta\phi}$ : Observable (1/2)

$$R_{\Delta\phi} = \frac{1}{N_{\text{jet}}(p_T)}$$

Number of jets in a jet  $p_T$  bin ( $\sim \alpha_s^2$  @LO)

2-jet topology	
 <p><math>R_{\Delta\phi}(p_T)</math> entries <math>\Delta\phi \approx \pi</math> Numerator: 0 Denominator: 2</p>	


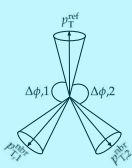
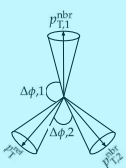
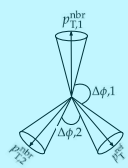
Definition inspired by  $D_0$ 's  $R_{\Delta_R}$  observable

# CMS - $R_{\Delta\phi}$ : Observable (1/2)

Jets with neighbours within azimuthal separation:  
 $2\pi/3 < \Delta\phi < 7\pi/8$  and  $p_T > 100$  GeV ( $\sim \alpha_s^3$  @LO)

$$R_{\Delta\phi} = \frac{\sum_{i=1}^{N_{\text{jet}}(p_T)} N_{\text{nbr}}^{(i)}(\Delta\phi, p_{T\text{min}}^{\text{nbr}})}{N_{\text{jet}}(p_T)}$$

Number of jets in a jet  $p_T$  bin ( $\sim \alpha_s^2$  @LO)

2-jet topology	3-jet topology (all jets with $p_T > 100$ GeV)		
 <p><math>R_{\Delta\phi}(p_T)</math> entries  <math>\Delta\phi \approx \pi</math>                      Numerator: 0                      Denominator: 2</p>	 <p>Numerator: 2  <math>2\pi/3 &lt; \Delta\phi,1 &lt; 7\pi/8</math>  <math>2\pi/3 &lt; \Delta\phi,2 &lt; 7\pi/8</math></p>	 <p>Numerator: 1  <math>2\pi/3 &lt; \Delta\phi,1 &lt; 7\pi/8</math>  <math>\Delta\phi,2 &lt; 2\pi/3</math></p>	 <p>Numerator: 1  <math>2\pi/3 &lt; \Delta\phi,1 &lt; 7\pi/8</math>  <math>\Delta\phi,2 &lt; 2\pi/3</math></p>
$R_{\Delta\phi}(p_T)$ entries + Numerator: 1     + Numerator: 1 $2\pi/3 < \Delta\phi,1 < 7\pi/8$ $2\pi/3 < \Delta\phi,1 < 7\pi/8$ $\Delta\phi,2 < 2\pi/3$ $\Delta\phi,2 < 2\pi/3$ Denominator: 3			

Definition inspired by  $D_0$ 's  $R_{\Delta_R}$  observable

# CMS - $R_{\Delta\phi}$ : Samples and event selection

## Data

**Full Run 2 (2016-2018)**  $\rightarrow \sqrt{s} = 13$  TeV,  
 $\mathcal{L}_{int} = 134 \text{ fb}^{-1}$

## Jet reconstruction (FASTJET)

- **Jet algorithm:** anti- $k_T$
- **Jet size:**  $R=0.7$

# CMS $-R_{\Delta\phi}$ : Samples and event selection

## Data

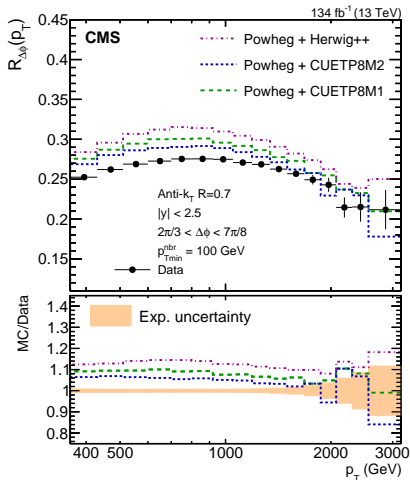
Full Run 2 (2016-2018)  $\rightarrow \sqrt{s} = 13$  TeV,  
 $\mathcal{L}_{int} = 134 \text{ fb}^{-1}$

## Jet reconstruction (FASTJET)

- Jet algorithm: anti- $k_T$
- Jet size:  $R=0.7$

## Event selection

- Phase space:
  - $p_T > 50$  GeV
  - $|y| < 2.5$
- Numerator criteria:
  - $(\Delta\phi_{\min}, \Delta\phi_{\max}) = (2\pi/3, 7\pi/8)$
  - $p_{T\min}^{\text{nbr}} = 100$  GeV



Powheg overestimates the measurement  
 $\rightarrow$  Fixed-order pQCD needed

# CMS - $R_{\Delta\phi}$ : Experimental uncertainties

Equivalent observable definition

$$\mathbf{R}_{\Delta\phi} = \frac{\sum_{i=1}^{N_{\text{jet}}(\mathbf{p}_T)} \mathcal{N}_{\text{nbr}}^{(i)}(\Delta\phi, \mathbf{p}_{T\text{min}}^{\text{nbr}})}{N_{\text{jet}}(\mathbf{p}_T)} = \frac{\sum_n n \mathcal{N}(\mathbf{p}_T, n)}{\sum_n \mathcal{N}(\mathbf{p}_T, n)}$$

- where  $n$  is the number of neighbours and  $\mathbf{p}_T$  is jet's transverse momentum.

# CMS - $R_{\Delta\phi}$ : Experimental uncertainties

Equivalent observable definition

$$R_{\Delta\phi} = \frac{\sum_{i=1}^{N_{\text{jet}}(p_T)} N_{\text{nbr}}^{(i)}(\Delta\phi, p_{T\text{min}}^{\text{nbr}})}{N_{\text{jet}}(p_T)} = \frac{\sum_n n N(p_T, n)}{\sum_n N(p_T, n)}$$

- where  $n$  is the number of neighbours and  $p_T$  is jet's transverse momentum.

✚ 2D unfolding of  $N(p_T, n)$  distribution.

✓ Migrations among  $p_T$  and among  $n$  bins.

✓ Account for non-trivial numerator-denominator correlations.

**Stat.:** 0.18 – 10.49 %

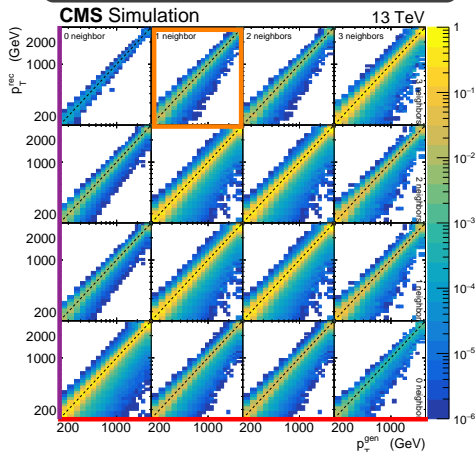
**JES:** 0.65 – 5.00 %

**JER:** 0.04 – 0.77 %

**Other:** < 1%

**⚠ All uncertainties remain below 1% up to 1.5 TeV**

Probability matrix for the 2D  $N(p_T, n)$

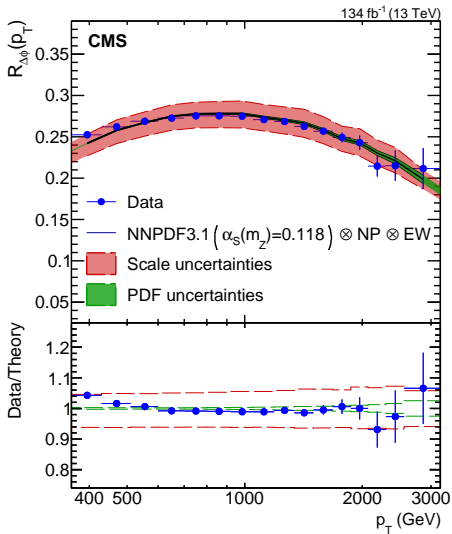


## Theoretical predictions

- Fixed-order predictions pQCD NLO
- NLOJET++ (up to 3 jets NLO)
- **fastNLO** framework
- $\mu_R = \mu_F = \hat{H}_T/2$  with  
$$\hat{H}_T = \sum_{i \in \text{partons}} p_{T,i}$$
- Separate calculation for numerator and denominator



# CMS - $R_{\Delta\phi}$ : Fixed-order pQCD



## Theoretical predictions

- Fixed-order predictions pQCD NLO
- NLOJET++ (up to 3 jets NLO)
- **fastNLO** framework
- $\mu_R = \mu_F = \hat{H}_T/2$  with  $\hat{H}_T = \sum_{i \in \text{partons}} p_{T,i}$
- Separate calculation for numerator and denominator

## Theoretical predictions for $R_{\Delta\phi}$

- Corrected for NP and EW
- Data-Theory agreement (within uncertainties)
- Uncertainties:
  - PDF: 1-2%
  - Scale: 2-8%

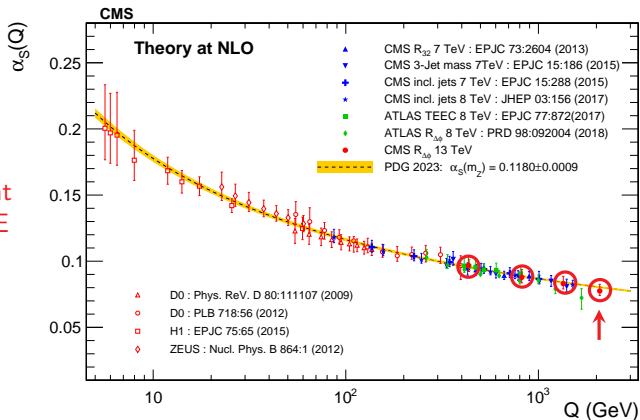
**⚠ NNLO predictions not yet available for  $R_{\Delta\phi}$  !**

# CMS - $R_{\Delta\phi}$ : Fixed-order pQCD

$R_{\Delta\phi}$  sensitive to  $\alpha_S$ :

$$\alpha_S(m_Z) = 0.117^{+0.0117}_{-0.0074}$$

- $\alpha_S(Q)$  results consistent with predictions by RGE
- Extended range up to  $\sim 2$  TeV



## Double-differential (2D)

- Inclusive double-differential dijet cross-section as function of maximum rapidity and the invariant mass of the two leading jets:

$$\frac{d^2\sigma}{dy_{\max} dm_{1,2}} = \frac{1}{\mathcal{L}_{int}} \frac{N_{eff}}{(2\Delta |y|_{\max}) \Delta m_{1,2}}$$

- $m_{1,2} = \sqrt{(E_1 + E_2)^2 - (\vec{p}_1 + \vec{p}_2)^2}$ ,  $|y|_{\max} = \max(|y_1|, |y_2|)$

# CMS - Dijet cross sections: Observable (2/2)

## Double-differential (2D)

- Inclusive double-differential dijet cross-section as function of maximum rapidity and the invariant mass of the two leading jets:

$$\frac{d^2\sigma}{dy_{\max} dm_{1,2}} = \frac{1}{\mathcal{L}_{int}} \frac{N_{eff}}{(2\Delta|y|_{\max})\Delta m_{1,2}}$$

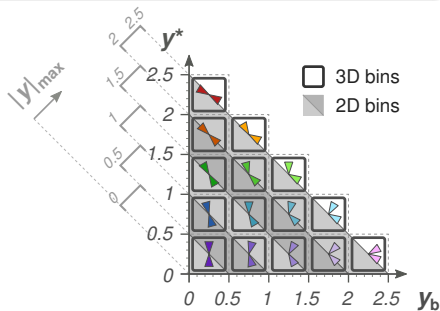
- $m_{1,2} = \sqrt{(E_1 + E_2)^2 - (\vec{p}_1 + \vec{p}_2)^2}$ ,  $|y|_{\max} = \max(|y_1|, |y_2|)$

## Triple-differential (3D)

- Inclusive triple-differential dijet cross-section as a function of  $y^*$ ,  $y_b$  and the invariant mass **or** average  $p_T$  of the two leading jets:

$$\frac{d^3\sigma}{dy^* dy_b dx} = \frac{1}{\mathcal{L}_{int}} \frac{N_{eff}}{\Delta y^* \Delta y_b \Delta x}$$

- $y^* = \frac{1}{2} |y_1 - y_2|$ ,  $y_b = \frac{1}{2} |y_1 + y_2|$
- $x = m_{1,2}$  or  $\langle p_T \rangle_{1,2} = \frac{1}{2} (p_{T,1} + p_{T,2})$



# CMS - Dijet cross sections: Samples and event selection

## Samples

**Data:** 2016

→  $\sqrt{s} = 13 \text{ TeV}$ ,  $\mathcal{L}_{int} = 36.3 \text{ fb}^{-1}$

## Jet reconstruction (FASTJET)

- **Jet algorithm:** anti- $k_T$
- **Jet sizes:**  $R=0.4$  and  $R=0.8$

## Samples

**Data:** 2016

→  $\sqrt{s} = 13$  TeV,  $\mathcal{L}_{int} = 36.3$  fb<sup>-1</sup>

## Jet reconstruction (FASTJET)

- **Jet algorithm:** anti- $k_T$
- **Jet sizes:** R=0.4 and R=0.8

## Event selection

- **Double-differential:**
  - $p_{T,1} \geq 100$  GeV ,  $p_{T,2} \geq 50$  GeV
  - $|y_1| < 2.5$  ,  $|y_2| < 2.5$
- **Triple-differential:**
  - $p_{T,1} \geq 100$  GeV ,  $p_{T,2} \geq 50$  GeV
  - $|y_1| < 3.0$  ,  $|y_2| < 3.0$

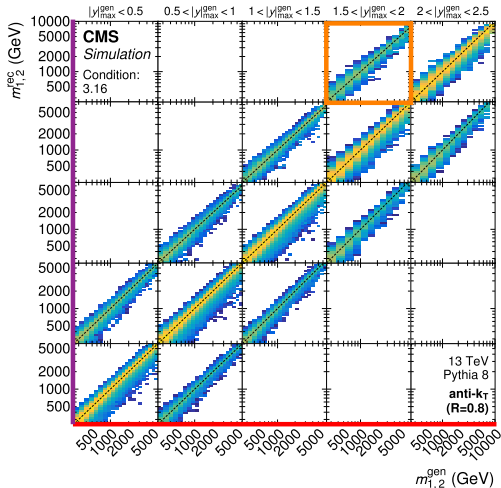
**⚠ Events from one measurement are not necessarily included in the phase space of the other!**

# CMS - Dijet cross sections: Unfolding

- Detector level  $\rightarrow$  Particle level spectrum
- Least-square minimisation:  $\chi^2 = (Ax + b - y)^T V_y^{-1} (Ax + b - y)$  (same method for  $R_{\Delta\phi}$ )

# CMS - Dijet cross sections: Unfolding

- Detector level  $\rightarrow$  Particle level spectrum
- Least-square minimisation:  $\chi^2 = (Ax + b - y)^T V_y^{-1} (Ax + b - y)$  (same method for  $R_{\Delta\phi}$ )



## 2-D Unfolding with TUNFOLD

Correct:

- $\rightarrow$  Background (Fake jets)
- $\rightarrow$  Unsmear detector effects
- $\rightarrow$  Inefficiencies (Miss jets)

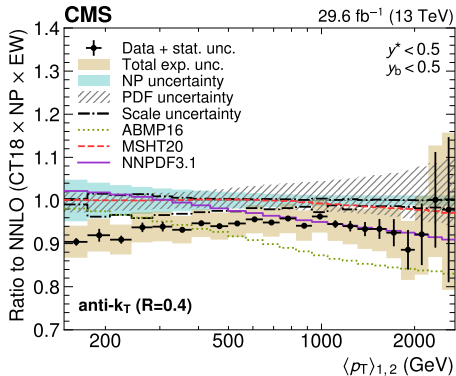
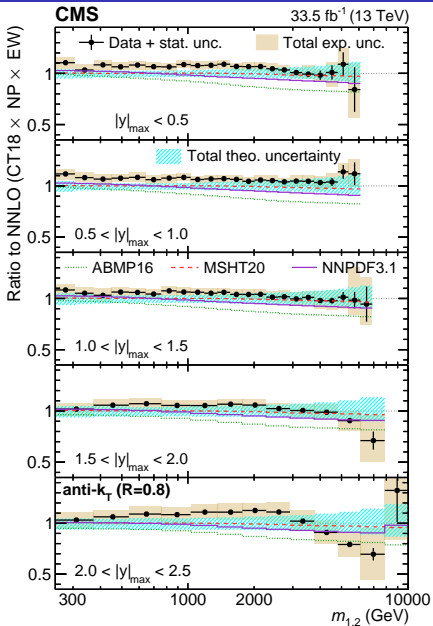
■ Matrix structure

- **x axis: generator-level  $m_{jj}$**
- **y axis: reconstructed-level  $m_{jj}$**
- **inner cells: different  $|y|_{max}$  bins**

■ Condition Number:  $CN = \left| \frac{\max\_eig}{\min\_eig} \right|$   
 $CN < 10 \rightarrow$  Acceptable unfolding performance

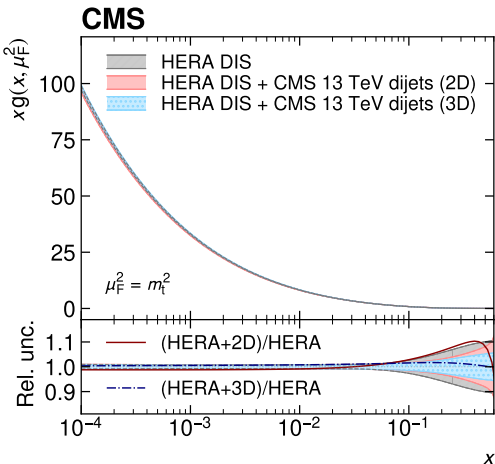


# CMS - Dijet cross sections: Fixed order pQCD



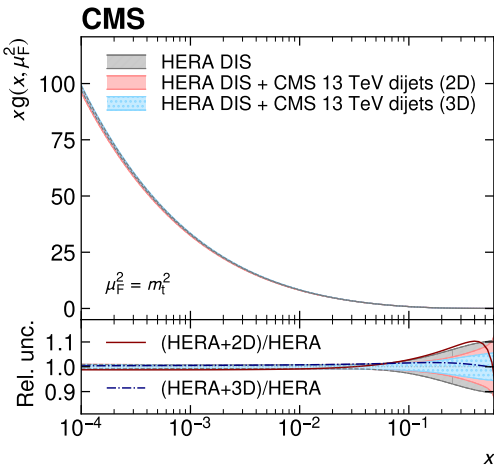
- Theory corrected for NP and EW effects
- Nice description of Data from CT18 (10%)
- Better Data-Theory agreement for AK8
- Comparison with other PDF sets

# CMS - Dijet cross sections: Fixed order pQCD



- Impact of measurement on PDFs
- Using HERA parametrisation
- Higher energy range of dijet mass  
→ included in fit
- $R = 0.8$  (better Data-Theory agreement)
- Shown here: gluon PDF
- Reduced uncertainties especially in high  $x$  region

# CMS - Dijet cross sections: Fixed order pQCD



- Impact of measurement on PDFs
- Using HERA parametrisation
- Higher energy range of dijet mass  
→ included in fit
- $R = 0.8$  (better Data-Theory agreement)
- Shown here: gluon PDF
- Reduced uncertainties especially in high  $x$  region
- Extraction of  $\alpha_S$ :

2D:  $\alpha_S(m_Z) = 0.1179 \pm 0.0019$  (tot.)

3D:  $\alpha_S(m_Z) = 0.1181 \pm 0.0022$  (tot.)

# Summary & Conclusions

ATLAS

- (A)TEEC<sup>1</sup>:
  - ✓ Precise determination of  $\alpha_S(m_Z)$  and running of  $\alpha_S(Q)$  in TeV scale
- Jet cross section ratios<sup>2</sup>:
  - ✓ Improvement of JES uncertainty
  - ✓ Is eligible for determination of  $\alpha_S(m_Z)$

---

<sup>1</sup>JHEP 07 (2023) 85

<sup>2</sup>arXiv:2405.20206, submitted to PRD

<sup>3</sup>EPJC 84, 842 (2024)

<sup>4</sup> arXiv:2312.16669, submitted to EPJC

# Summary & Conclusions

ATLAS

- (A)TEEC<sup>1</sup>:
  - ✓ Precise determination of  $\alpha_S(m_Z)$  and running of  $\alpha_S(Q)$  in TeV scale
- Jet cross section ratios<sup>2</sup>:
  - ✓ Improvement of JES uncertainty
  - ✓ Is eligible for determination of  $\alpha_S(m_Z)$

CMS

- Azimuthal correlations ( $R_{\Delta\phi}$ )<sup>3</sup>:
  - ✓ Small experimental uncertainties → appealing for  $\alpha_S(m_Z)$  determination using NNLO
  - ✓ Investigation of  $\alpha_S(Q)$  running in the TeV region, expanding the range of the running
- Multi-differential dijet cross sections<sup>4</sup>:
  - ✓ Improved determination of PDFs compared to fits from HERA data alone
  - ✓ Precise determination of  $\alpha_S(m_Z)$  value

---

<sup>1</sup>JHEP 07 (2023) 85

<sup>2</sup>arXiv:2405.20206, submitted to PRD

<sup>3</sup>EPJC 84, 842 (2024)

<sup>4</sup> arXiv:2312.16669, submitted to EPJC

**THANK YOU FOR YOUR  
ATTENTION**

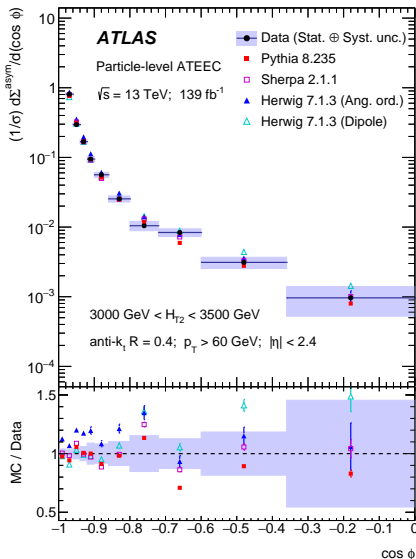
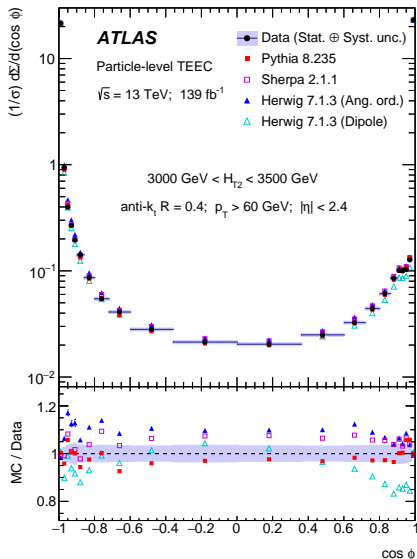
# BACK UP

# (A)TEEC: Systematic uncertainties

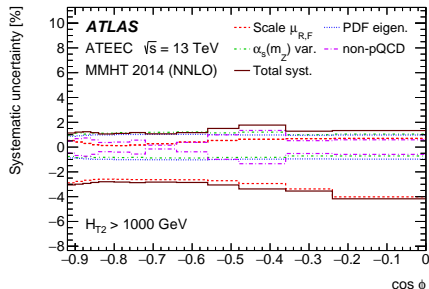
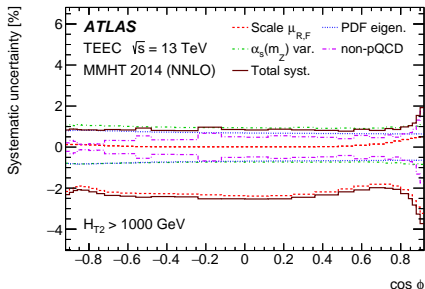
- **Jet Energy Scale(JES)**: restores energy of rec. jets by scaling  $p_T$ , energy, mass
- **Jet Energy Resolution (JER)**: differences in response in Data and MC by imperfect simulation  $\rightarrow$  smearing energy of jets in MC:  $c = \mathcal{R}_{in\ situ}^{data} / \mathcal{R}_{in\ situ}^{MC}$
- **Jet Angular Resolution (JAR)**: smearing  $\phi$  by resolution in MC ( $p_T$  constant)
- **Unfolding**: mismodelling of data by simulation, difference between unfolded and generator level MC distribution
- **Modelling**: difference between unfolded cross sections of MC samples



# (A) TEEC: Particle level measurement



# (A) TEEC: Theoretical uncertainties



**Total: 1.0-3.5%**

**$\alpha_S$  var.: 0.8-1%**

**NP: 0.3-1.8%**

- **Scale:** calculated by considering independent variations of  $\mu_f$  and  $\mu_r$

- **PDF:** obtained by considering the set of eigenvectors/replicas provided by each PDF group

- **Non-perturbative:** extracted from the envelope of the differences from different MC predictions

- **$\alpha_S$  variation:** effect of varying  $\alpha_S(m_Z)=0.117-0.119$

**Scale: 0.5-3.3%**

**PDF  $\approx 0.8\%$**

**Total: 1.0-4.2%**

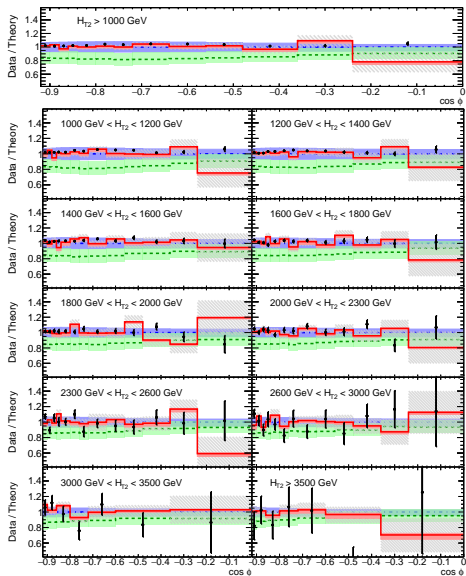
**$\alpha_S$  var.: 0.5-1%**

**NP: 0.5-1.5%**

**Scale: 0.5-4%**

**PDF:  $\approx 1\%$**

# (A) TEEC: Fixed-order pQCD



**ATLAS**

Particle-level ATEEC

$\sqrt{s} = 13 \text{ TeV}; 139 \text{ fb}^{-1}$

anti-k,  $R = 0.4$

$p_T > 60 \text{ GeV}$

$|\eta| < 2.4$

$\mu_{R,F} = \hat{A}_T$

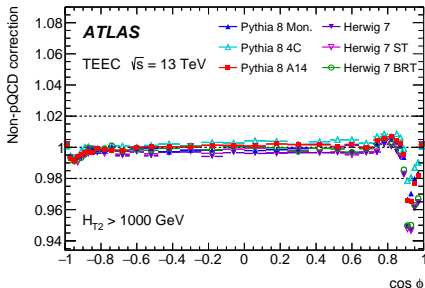
$\alpha_s(m_Z) = 0.1180$

MMHT 2014 (NNLO)

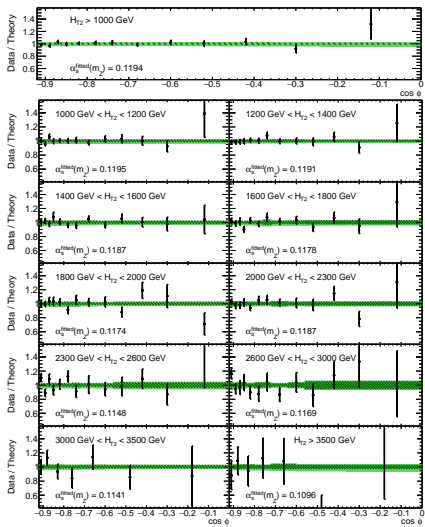
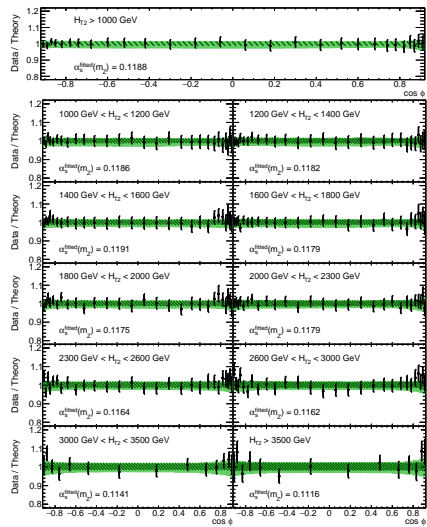
— Data  
 - - - LO  
 ■ NLO  
 ■ NNLO

Nice Data - Theory agreement within uncertainties

- NP corrections from several MC event generators
- Value of NP factors around unity



# (A) TEEC: Data Ratio to fitted Theory



**ATLAS**

Particle-level ATEEC

$\sqrt{s} = 13 \text{ TeV}; 139 \text{ fb}^{-1}$

anti- $k_R$   $R = 0.4$

$p_T > 60 \text{ GeV}$

$|\eta| < 2.4$

$\mu_{R,F} = \hat{P}_T$

NNLO pQCD

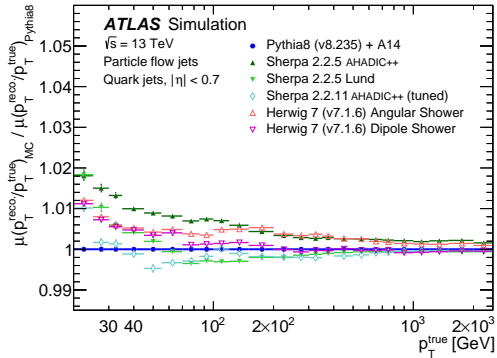
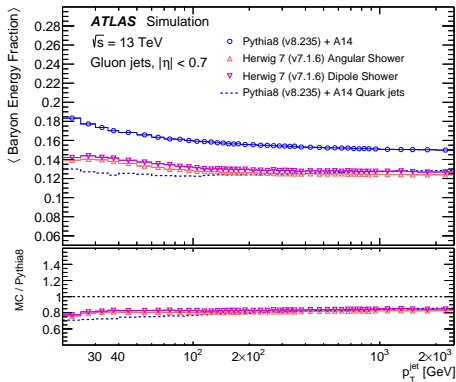
MMHT 2014 (NNLO)

— Exp. unc.

/// Non-scale unc.

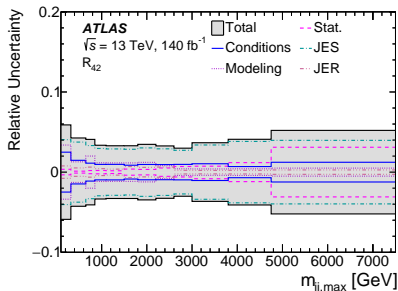
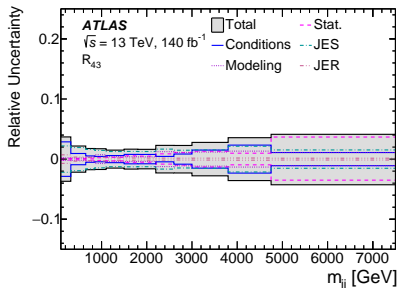
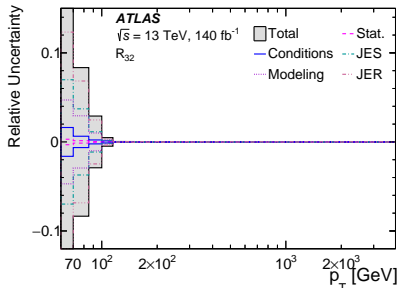
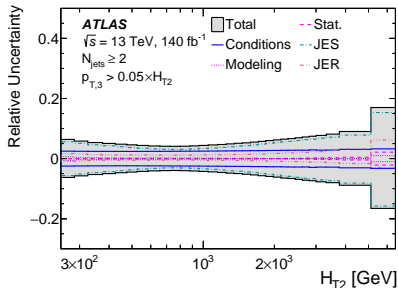
■ Theo. unc.

# Cross section ratios: Precision study

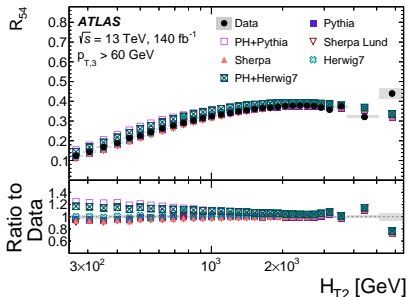
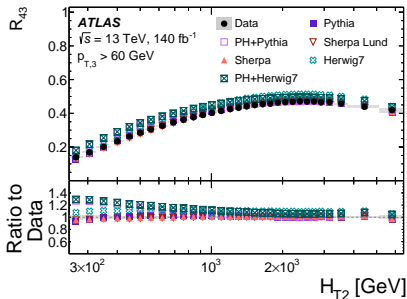
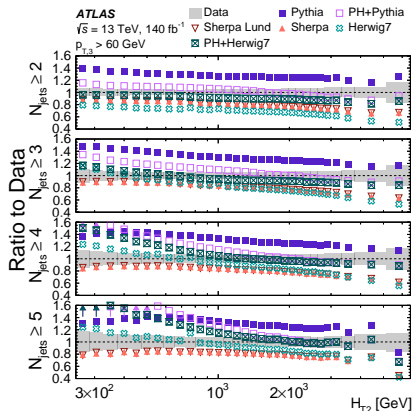


Parton Shower model in HERWIG models  
does not affect the distribution much

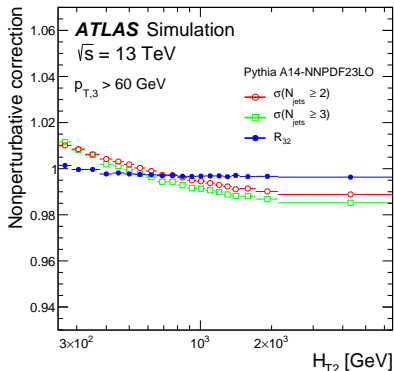
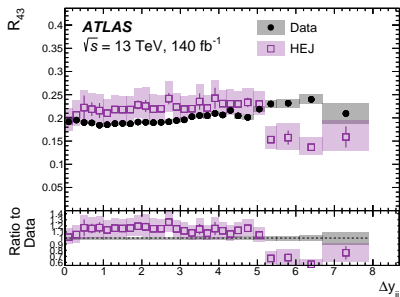
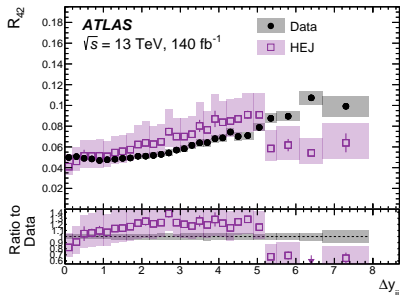
# Cross section ratios: JES



# Cross section ratios: Comparison to MC



# Cross section ratios: Fixed-order pQCD



NP deviate from unity by:

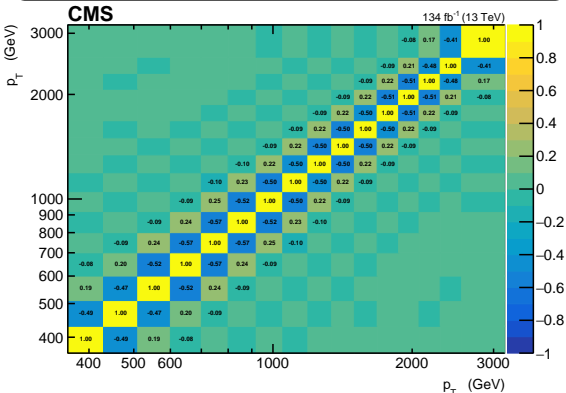
- 2% for 2 and 3 jet cross sections
- 0.5% for  $R_{32}$

Uncertainty smaller than 0.5%



# $R_{\Delta\phi}$ : Experimental uncertainties

Statistical correlation matrix for  $R_{\Delta\phi}$  after unfolding



- **Statistical:** from the covariance matrix *after* unfolding
- Correlations are considered in statistical uncertainty
- Diagonal elements: unity by construction (a bin is fully correlated with itself)
- Off-diagonal elements: bin-to-bin (anti-correlations)

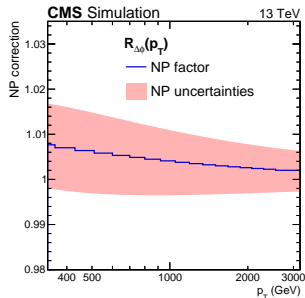
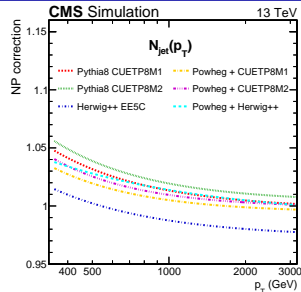
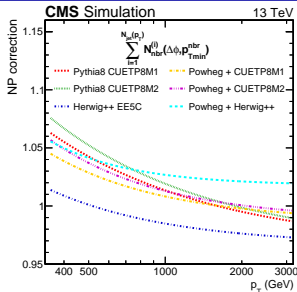
- **Statistical:** from the covariance matrix *after* unfolding
- **JES:** Jet Energy Scale uncertainty sources  
→  $p_T = p_T(1 \pm \text{unc. source})$
- **JER:** Jet Energy Resolution smearing process applied to MC samples
- **Other:** Prefiring corrections, PU profile reweighting, MC modeling

# $R_{\Delta\phi}$ : NP corrections

- NP correction factors:

$$C^{\text{NP}} = \frac{\sigma^{\text{PS+MPI+HAD}}}{\sigma^{\text{PS}}}$$

- Parametrisation of  $C^{\text{NP}}$  with simple polynomial function  $a + b \cdot p_T^c$
- Envelope from the predictions of the different MC event generators.
- Corrections of fixed-order pQCD predictions (parton level) for non-perturbative (NP) effects of multiple parton interactions (MPI) and hadronization (HAD)
- Applied on theory to be compatible with particle-level measurement



# $R_{\Delta\phi}$ : ElectroWeak corrections

## Full NLO corrections to 3-jet production and $R_{32}$ at the LHC

M. Reyer, M. Schönherr, S. Schumann [arXiv:1902.01763](https://arxiv.org/abs/1902.01763)  $\rightarrow \mathcal{O}(\alpha_s^n \alpha^m)$ , with  $n + m = 2$  and  $n + m = 4$ .

### Combination of QCD and EW corrections

#### Pure NLO EW corrections for n-jet:

$$\sigma_{nj}^{\text{NLO EW}} = \sigma_{nj}^{\text{LO}} + \sigma_{nj}^{\Delta\text{NLO}_1}$$

$\Delta\text{NLO}_1$ : virtual and real EW corrections.

#### Combination to QCD process:

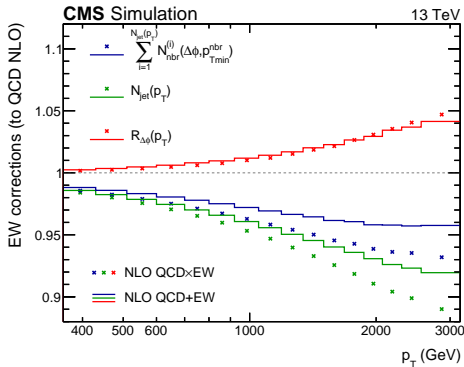
① Additive:  $\sigma_{nj}^{\text{NLO QCD+EW}}$

$$\sigma_{nj}^{\text{LO}} + \sigma_{nj}^{\Delta\text{NLO}_0} + \sigma_{nj}^{\Delta\text{NLO}_1}$$

$\Delta\text{NLO}_0$ : virtual and real QCD corrections.

② Multiplicative:  $\sigma_{nj}^{\text{NLO QCD}\times\text{EW}}$

$$\sigma_{nj}^{\text{LO}} \left( 1 + \frac{\sigma_{nj}^{\Delta\text{NLO}_0}}{\sigma_{nj}^{\text{LO}}} \right) \left( 1 + \frac{\sigma_{nj}^{\Delta\text{NLO}_1}}{\sigma_{nj}^{\text{LO}}} \right)$$



EW corrections for  $R_{\Delta\phi} < 5\%$  and  
EW correction uncertainties  $< 0.6\%$ .

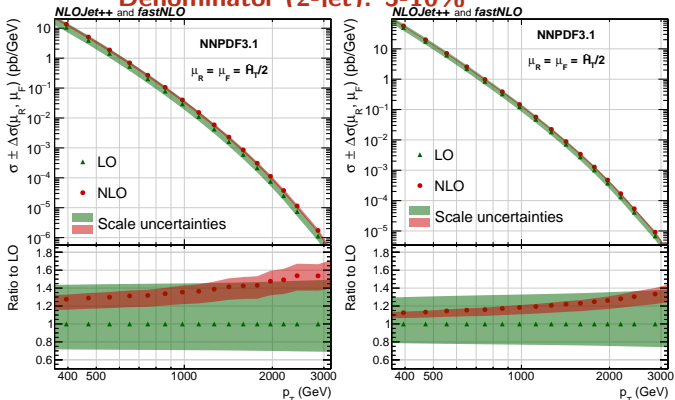
# CMS - $R_{\Delta\phi}$ : Fixed-order pQCD

- 4 NLO PDF sets (LHAPDF)
- PDF uncertainties: 68% CL Hessian/MC methods
- Scale uncertainties: difference between prediction for varying  $\frac{1}{2} \leq \mu_R, \mu_F \leq 2$

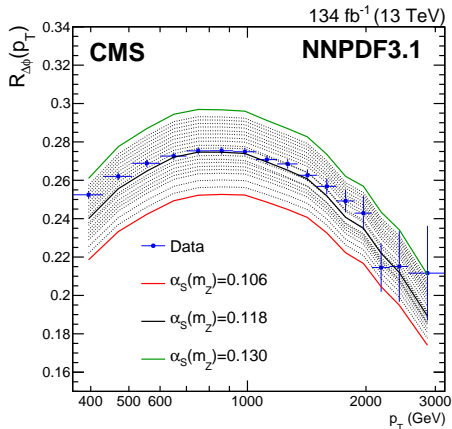
NLO scale uncertainties

Numerator (3-jet): 9-17%

Denominator (2-jet): 5-10%

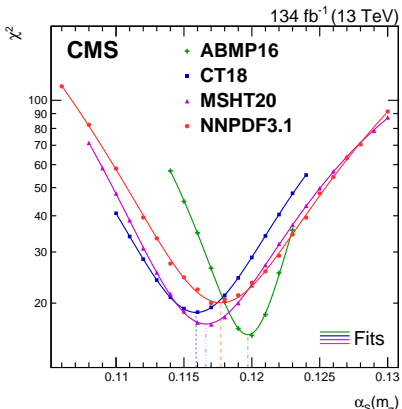


# $R_{\Delta\phi}$ : Sensitivity of $\Delta\phi$ to $\alpha_s(m_Z)$



- Particle-level Data with Theory corrected for NPs and EW
- Slight change in  $\alpha_s$  value from theory  $\rightarrow$  significantly different prediction
- Thus,  $R_{\Delta\phi}$  sensitive to  $\alpha_s$

# $R_{\Delta\phi}$ : Determination of $\alpha_s(m_Z)$



- **Extracted  $\alpha_s(m_Z)$  are compatible among each other within uncertainties.**

- **Scale uncertainties (theoretical) by far the dominant: 4 – 10 %.**

PDF set	$\alpha_s(m_Z)$	Exp	NP	PDF	EW	Scale	Total	$\chi^2/n_{dof}$
ABMP16	0.1197	0.0008	0.0007	0.0007	0.0002	+0.0043 -0.0042	+0.0045 -0.0044	16/16
CT18	0.1159	0.0013	0.0009	0.0014	0.0002	+0.0099 -0.0067	+0.0101 -0.0070	19/16
MSHT20	0.1166	0.0013	0.0008	0.0010	0.0003	+0.0112 -0.0063	+0.0114 -0.0066	17/16
NNPDF3.1	0.1177	0.0013	0.0011	0.0010	0.0003	+0.0114 -0.0068	+0.0116 -0.0071	20/16

## Least square minimisation

$$\chi^2 = \sum_{ij}^N (D_i - T_i) C_{ij}^{-1} (D_j - T_j)$$

$N$ : number of measurements

$D_i$ : experimental data

$T_i$ : theoretical predictions

$C_{ij}$ : covariance matrix

- **Covariance matrix composition:**

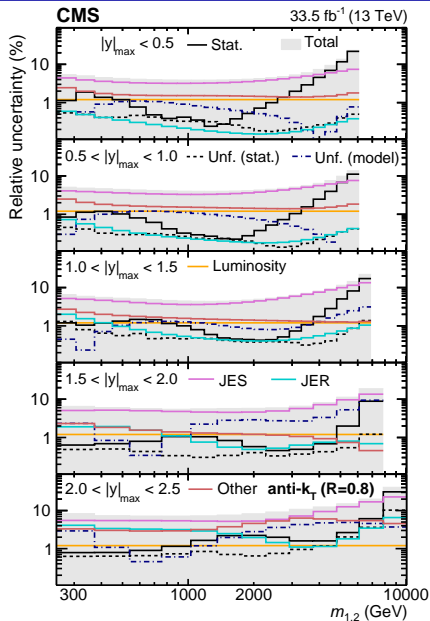
$$C_{ij} = C_{\text{uncor}} + C_{\text{exp}} + C_{\text{theo}}$$

$C_{\text{uncor}}$ : numerical precision of FO predictions

$C_{\text{exp}}$ : all the experimental uncertainties

$C_{\text{theo}}$ : all the theoretical uncertainties

# Dijet cross sections: Experimental uncertainties



**JES:** 3 → 23%

**JER:**  $< 1 \rightarrow 7\%$

**Luminosity:** 1.2%

**Unfolding:**  $\sim 1\%$

in forward region: 3-6%

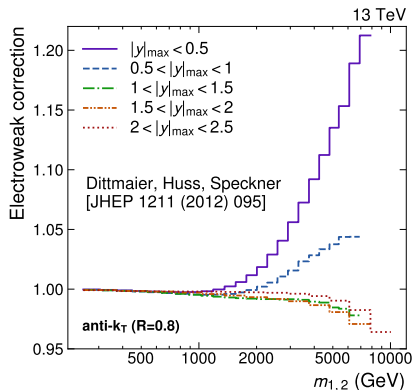
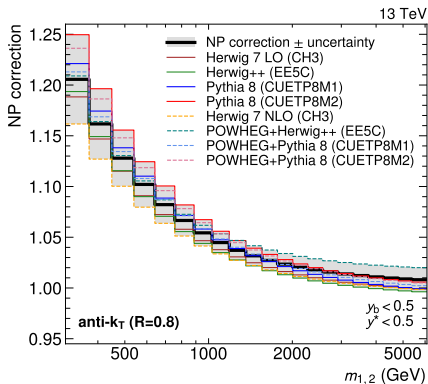
**Stat:**  $< 1 \rightarrow 31\%$

(larger in high  $m_{jj}$  bins)

**Total:** 4 → 41%

(quadratic sum of contribution from all uncertainty sources)

# Dijet cross sections: NP and EW corrections



- $C_{NP} = \frac{\sigma^{PS+HAD+MPI}}{\sigma^{PS}}$
- Parametrise following  $a/x^b + c$  to mitigate fluctuations
- Large correction values in lowest  $m_{1,2}$  bins (up to 20%)

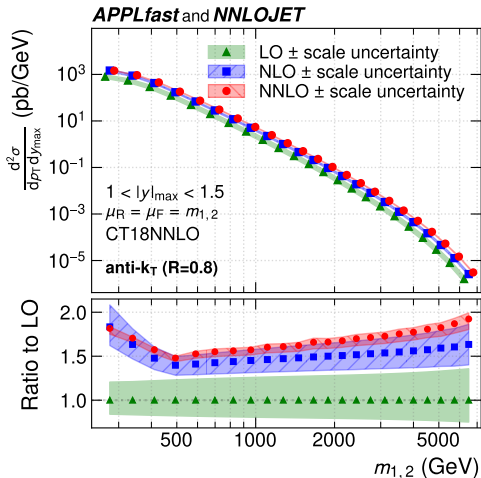
- EW effects become
- Larger EW factors for high  $m_{1,2}$  values and central  $|y|_{max}$  regions (Up to 15%)
- Forward  $|y|_{max}$  regions: negative EW factors



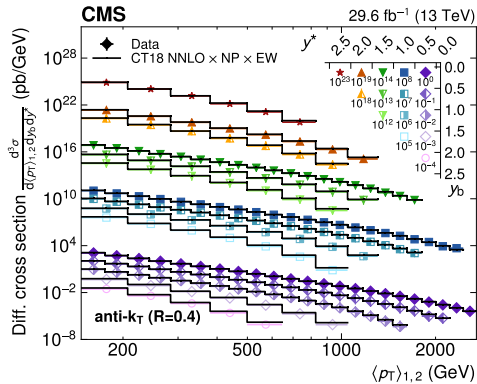
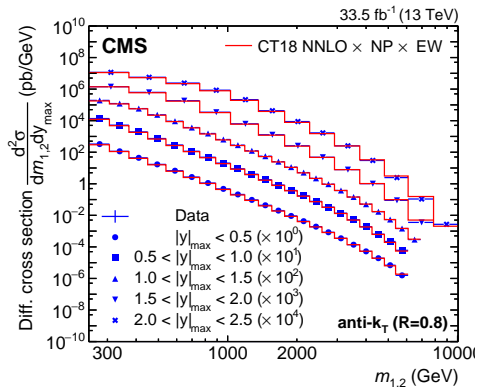
# Dijet cross sections: Fixed-order pQCD

## Theoretical predictions

- Up to NNLO in pQCD with NNLOJET (interfaced to FASTNLO via APPLFAST)
- $\mu_R = \mu_F = m_{1,2}$
- **PDF set:** CT18 NNLO
- Band from NNLO corrections mostly lies within the NLO, showing good perturbative convergence.

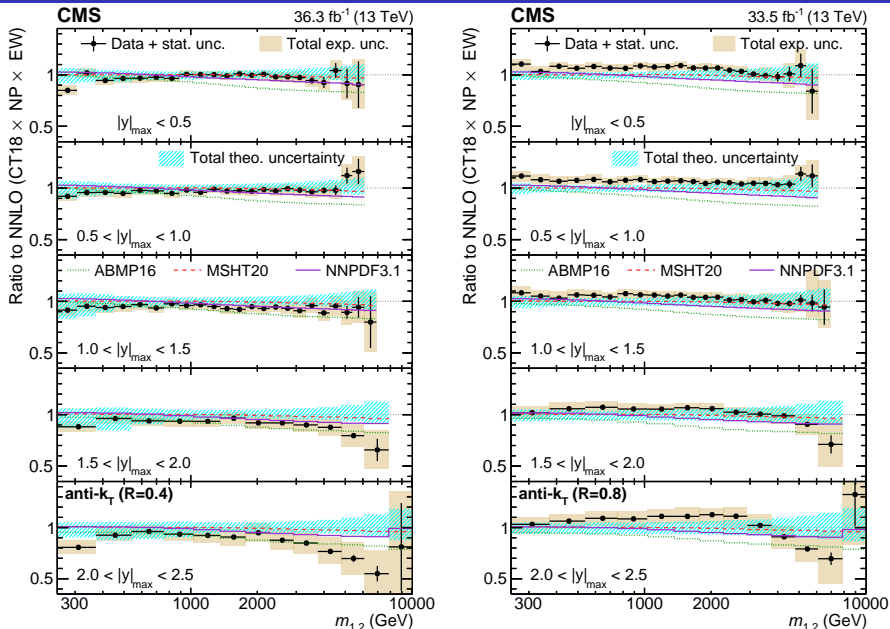


# Dijet cross sections: Fixed order pQCD

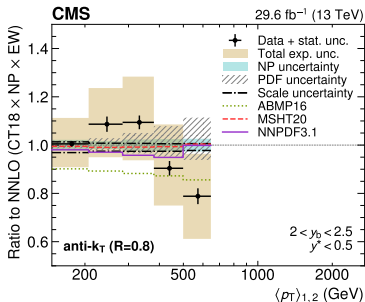
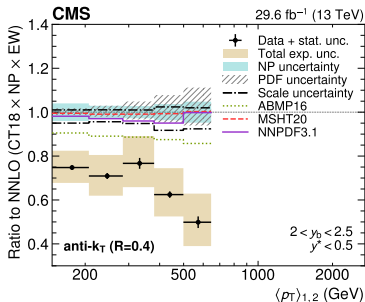
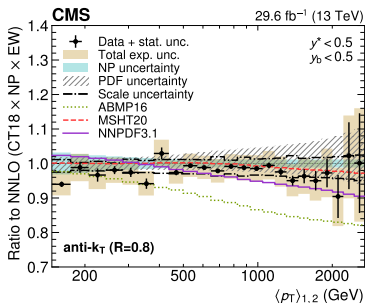
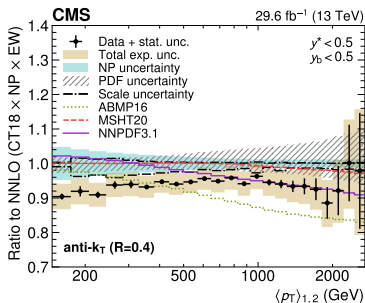


- Fixed-order pQCD predictions at NNLO corrected with NP and EW
- Shown here: Data and CT18

# Dijet cross sections: Data - Theory comparison (2D)



# Dijet cross sections: Data - Theory comparison (3D)



# Dijet cross sections: HERA fits

